

# Implementing a Dynamic Stall Model for Airfoils with Deformable Trailing Edges

Peter Bjørn Andersen<sup>[I]</sup>  
Mac Gaunaa<sup>[II]</sup>  
Christian Bak<sup>[III]</sup>  
Morten Hartvig Hansen<sup>[IV]</sup>

**[Abstract]** The present work contains an extension of the Beddoes-Leishman type dynamic stall model. In this work a Deformable Trailing Edge Geometry has been added to the dynamic stall model. The model predicts the unsteady aerodynamic forces and moments on an airfoil section undergoing arbitrary motion in heave, lead-lag, pitch and trailing edge flapping. In the linear region, the model reduces to the inviscid model which includes the aerodynamic effect of a thin airfoil with a deformable camberline in inviscid flow. The proposed model can be considered an amalgamation between: a modal expanded inviscid thin airfoil; and a traditional dynamic stall model with the effects of a dynamic boundary layer and turbulent flow separation. Furthermore, 2D measurements from an open wind tunnel will be used as input for the model. **Keywords:** Dynamic Stall, Trailing edge flap

## Nomenclature

AOA	= Angle Of Attack, Airfoil inflow angle
$A_i, b_i$	= $A_i$ and $b_i$ are profile specific constants for near wake state variables
$\alpha$	= AOA
$\alpha_{0,st}^\beta$	= Equivalent AOA shift in attached flow lift curve due to a static $\beta$ deflection angle
$\alpha_{0,dyn}^\beta$	= Equivalent AOA shift in attached flow lift curve due to the first $\beta$ derivative
$\alpha_0^c$	= Equivalent AOA shift in attached flow lift curve due to a cambered profile
$\alpha_0$	= Sum of $\alpha_{0,dyn}^\beta$ , $\alpha_{0,st}^\beta$ and $\alpha_0^c$
$\alpha_{3/4}$	= Geometrical angle of attack at the three-quarter point
$\alpha_E$	= Effective geometric AOA using the retarding unsteady near wake effects from the shed vortexes
$\alpha_{o,E}$	= Effective equivalent AOA shift with retarding unsteady near wake effects from the shed vortexes
$\beta$	= DTEG deflection angle
$b$	= Airfoil half chord
$c$	= Airfoil chord
$C_{D0}$	= Drag coefficient at zero lift
$\Delta C_{D,DTEG}$	= Drag contribution from the DTEG
$C_D^{dyn}$	= Dynamic drag coefficient
$C_L^p$	= The attached flow unsteady lift
$C_L^{p,c}$	= Helping state variable which is the lift coefficient after the pressure time-lag is included
$C_L^{st}$	= Stationary lift as function of AOA
$C_L^{fs}$	= Fully separated lift (stationary) as function of AOA
$C_{L,\alpha}$	= Lift slope for attached flow regime

---

[I] Ph.D student, Risø-DTU, DK-4000, Denmark. Email: [peter.bjoern.andersen@risoe.dk](mailto:peter.bjoern.andersen@risoe.dk)

[II] Senior Scientist, Risø-DTU, DK-4000, Denmark. Email: [mac.gaunaa@risoe.dk](mailto:mac.gaunaa@risoe.dk)

[III] Senior Scientist, Risø-DTU, DK-4000, Denmark. Email: [christian.bak@risoe.dk](mailto:christian.bak@risoe.dk)

[IV] Senior Scientist, Risø-DTU, DK-4000, Denmark. Email: [morten.hartvig.hansen@risoe.dk](mailto:morten.hartvig.hansen@risoe.dk)

$C_L^{\text{dyn}}$	= Dynamic lift as function of AOA and DTEG deflection angle.
$\Delta C_{L,\text{DTEG}}$	= Lift contribution from DTEG
$C_{M_0}$	= Moment coefficient at zero lift
$C_M$	= Moment coefficient
DTEG	= Deformable TE Geometry
$\varepsilon$	= Parameter following the DTEG camberline.
$f^{\text{dyn}}$	= Dynamic separation point values between one and zero.
$f^{\text{st}}$	= Stationary separation point values between one and zero.
$H_{\text{dydx}}, H_y$	= Deflections integrals used by DTEG dynamics
$k$	= Reduced frequency $k = \omega b/U$
$\tau_p, \tau_b$	= Dynamic pressure-lift time lag and buildup/destruction time lag for the boundary layer
TE	= Trailing Edge
$U, U_0, U$	= Free-stream air velocity ( $U_x, U_y$ are coordinate components of $U$ )
$\omega$	= Frequency in radians pr. second
$w$	= Three-quarter point downwash
$w_\beta$	= Three-quarter point downwash contribution from DTEG
$w_{3/4}$	= Three-quarter point downwash contribution from airfoil
$x, y, z$	= Local coordinates used to describe DTEG
$x_i, y_i, z_i$	= Indicial state variables for the near wake history

## I. Introduction

Adding a TE flap to a wing is a well known method for changing the aerodynamic pressure distribution around the wing. TE flap devices are used for noise and vibration reductions on rotorcrafts. Extensive works have been conducted in this area and the authors refer to the review paper by Friedmann<sup>[1]</sup> for more details. At Risø-DTU National Laboratory for Renewable Energy, Denmark, a continuous research of using DTEG for reducing load fluctuations on wind turbines have been carried out<sup>[2-6]</sup>. For the purpose of this paper the flap or the DTEG is characterized by a smooth and continuous gradient from the non-deformable part of the airfoil to the deformable part. Furthermore, the part of the DTEG closest to the trailing edge has the largest structural rotations and at the point where the DTEG is fixed to the non-deformable part of the airfoil there is no structural rotation. This type of DTEG was chosen in Risø's previous work because flow separation and thereby corresponding noise and drag are reduced, compared to the rigid flap. Recent works have shown that the potential fatigue load reduction by use of DTEG may be greater than for traditional pitch control methods. By enabling the trailing edge to move independently and quickly along the radial position of the blade, local fluctuations in the aerodynamic forces can be compensated for by deformation of the airfoil geometry. Using a simplified aeroelastic model of a Vestas V66 wind turbine Andersen<sup>[5]</sup> found that the equivalent flapwise blade root moment could be reduced 60% for inflow with 10% turbulence using 7 meter adaptive DTEG on the 33-m blade. In Figure 1 an airfoil with a DTEG is shown with the DTEG in three different positions.

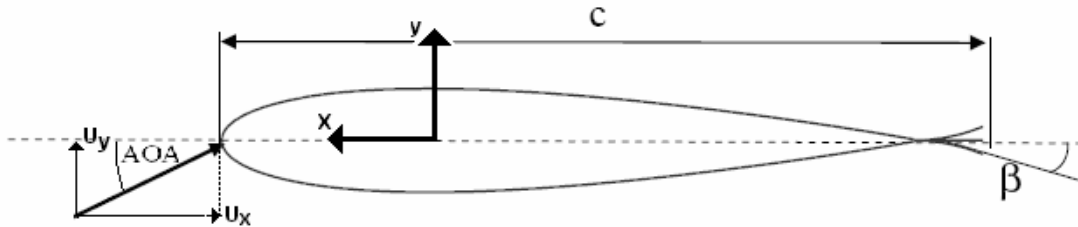


**Figure 1;** notation of an airfoil equipped with DTEG of the flap type. Local coordinate system follows  $c/4$  as illustrated. Three different positions of the DTEG are shown.

The notation connected to the airfoil geometry is shown, where AOA is the angle of attack of the incoming flow to the undeformed DTEG,  $\beta$  is the angle from the point where the DTEG is fixed on the non-deformable part of the airfoil to the trailing edge positive towards the pressure side. The free-stream air velocity is denoted  $\bar{U} = \sqrt{U_x^2 + U_y^2}$ . All previous

work investigating active load reduction using DTEG carried out at Risø National Laboratory has employed the aerodynamic model of Gaunaa<sup>[4]</sup>, which is an inviscid model. Therefore, the investigations have been confined to angles of attack in the linear region, where effects of stall are not present. Due to the great load reduction potential revealed previously, further investigations closer to and somewhat into the stalled region is needed. The present work contains an extension of the Beddoes-Leishman (B-L) type dynamic stall model, as described by Hansen<sup>[7]</sup> with the static and dynamic effect of a DTEG. The model predicts the unsteady aerodynamic forces and moments on an airfoil section undergoing arbitrary motion in heave, lead-lag, pitch and trailing edge (TE) flapping, and includes the effect of shed vorticity from the trailing edge and the effect of an instationary TE separation point. In the linear region, the model reduces to the inviscid model of Gaunaa. Therefore, the proposed model can be considered a crossover between the work of Gaunaa for the attached flow region and Hansen for the separated flow region and will make the aerodynamic forces a function of angle of attack (AOA) and deflection of the flap ( $\beta$ ). The range of the TE deflection is limited to +/- 5 degrees, the model is not expected handle large TE deflections e.g. 30-45 degrees. The model will be validated against wind tunnel measurements from Velux as described by Bak<sup>[8]</sup>.

## II. Theoretical model

The model consists of two parts; an inviscid and a viscous and part. In the inviscid part the airfoil is represented by its camberline with a mounted DTEG also represented by a camberline. The influence from the shed vorticity in the wake is described by a series of time-lags as used by Hansen<sup>[7]</sup> and Gaunaa<sup>[4]</sup>, in which the time-lag is approximated using an indicial function first outlined by Von Karman<sup>[9]</sup>, making the practical calculation of the aerodynamic response numerically very efficient by use of Duhamel superposition. In the viscous part of the model the dynamic behavior of the trailing edge (TE) separation is likewise modeled using an assumed time-lag between pressure distribution and lift and a time-lag for the separation point in the dynamic boundary layer. Using the same conditions as specified by Hansen<sup>[7]</sup> the TE separation is considered under stalled conditions. This chapter will deal with integrating the DTEG into the dynamic stall model by first describing parts of the DTEG model by Gaunaa<sup>[4]</sup> then implementing this into an attached flow formulation, then a fully separated flow formulation and finally the dynamics for the TE separation will be formulated.

### A. DTEG modeling basics

Based on the work of Gaunaa, the lift, drag and moment can be found for an airfoil using a series of modeshapes which model an unsteady camberline. A single modeshape, can be used to model the camberline of a DTEG undergoing unsteady deformations. Actuating the DTEG causes a change in the equivalent three-quarter downwash. The equivalent three-quarter point downwash for an airfoil with a DTEG is marked  $Q$  in the work of Gaunaa, whereas, the downwash will be called  $w_\beta$  in the present work and only represent the DTEG contribution to the downwash. It should be noted that  $w_\beta$  (or  $Q$ ) is not a physical property but should be regarded as a useful numerical number for determining the effect of TE shed vortices. For steady conditions using a single deformation modeshape,  $w_\beta$  is given by

$$\frac{w_\beta}{U} = -\frac{H_{dyd\epsilon}}{2\pi} \beta - \frac{H_y}{2\pi U} \frac{\partial \beta}{\partial t} \quad (1)$$

The deflection integrals  $H_y$  and  $H_{dyd\epsilon}$  are given by (2) and (3). Please note that the lower bound of 0.8 used in the integrals marks the start of a DTEG with a chordwise length of 10%.

$$H_y = -2 \int_{0.8}^1 \frac{y(x) \sqrt{1-x^2}}{x-1} dx \quad (2)$$

$$H_{dyd\epsilon} = -2 \int_{0.8}^1 \frac{\frac{\partial y}{\partial \epsilon}(\epsilon(x)) \sqrt{1-x^2}}{x-1} dx \quad (3)$$

The  $w_\beta$  is a useful quantity for finding the DTEG contribution to lift, drag and moment which has been derived by Gaunaa and shown in Appendix A for the simple one modeshape representation of a DTEG camberline. In some cases, empirical data for the DTEG is known e.g. from wind tunnel measurements. Appendix B shows the DTEG static lift  $\Delta C_{L,DTEG}^{st}(\alpha,\beta)$  curve from a measurement campaign using a Risø B1-18 profile. It is possible to introduce the empirical term  $\Delta C_{L,DTEG}^{st}$  by replacing the theoretical  $H_{dydx}$ . Keeping in mind that AOA ( $\alpha$ ) correlates proportional with the downwash ( $w$ ) by  $w = \overline{U}\alpha$ , the downwash elements of Equation (1) can be represented by an AOA representation given by

$$\alpha_{0,st}^\beta = \frac{H_{dydx}}{2\pi} \beta \cong \frac{\Delta C_{L,DTEG}(\alpha_0^c, \beta)}{C_{L,\alpha}} \quad (4)$$

$$\alpha_{0,dyn}^\beta = \frac{H_y}{2\pi U} \frac{\partial \beta}{\partial t}$$

where the term  $C_{L,\alpha}$  marks the attached lift slope at zero DTEG deflection  $\beta$ . The term  $\alpha_{0,st}^\beta$  is an equivalent AOA shift in attached flow lift curve due to a static  $\beta$  deflection angle and  $\alpha_{0,dyn}^\beta$  marks the contribution from the first  $\beta$  derivative to  $w_\beta$  given by Equation (1). Using Equation (4) the overall lift offset represented by a shift in AOA ( $\alpha_0$ ) due to a chambered profile and the use of a DTEG becomes equal to Equation (5).

$$\alpha_0 = \alpha_{0,st}^\beta + \alpha_{0,dyn}^\beta + \alpha_0^c \quad (5)$$

The term  $\alpha_0^c$  is the offset at zero lift due to a standard cambered profile.

## B. Lift in attached flow using the B-L and DTEG model

As in the original work of B-L a geometrical angle of attack at the three-quarter point  $\alpha_{3/4}$  will be formulated as

$$\alpha_{3/4} = \frac{w_{3/4}}{U} \quad (6)$$

The three-quarter point downwash without the influence of a DTEG is given by the variable  $w_{3/4}$ . The effective geometric AOA ( $\alpha_E$ ) is found using the retarding unsteady wake effects from the shed vortices as previously described using the Duhamel integral formulation. The profile has an unsteady camberline due to the added DTEG, which causes  $\alpha_0$  to be instationary. The unsteady offset of AOA  $\alpha_0$  is called  $\alpha_{0,E}$ . The unsteady DTEG deflection angle ( $\beta_E$ ) is based on the static DTEG deflection angle ( $\beta$ ) using the same integral formulation.

$$\alpha_E = \alpha_{3/4} \left( 1 - \sum_i A_i \right) + \sum_i x_i$$

$$\alpha_{0,E} = \alpha_0 \left( 1 - \sum_i A_i \right) + \sum_i y_i \quad (7)$$

$$\beta_E = \beta \left( 1 - \sum_i A_i \right) + \sum_i z_i$$

The indicial state variables for the wake history is given by

$$\begin{aligned}
x_i &= x_i \cdot e^{-ds \cdot b_i} + A_i \alpha_{3/4} (1 - e^{-ds \cdot b_i}) \\
y_i &= y_i \cdot e^{-ds \cdot b_i} + A_i \alpha_0 (1 - e^{-ds \cdot b_i}) \\
z_i &= z_i \cdot e^{-ds \cdot b_i} + A_i \beta (1 - e^{-ds \cdot b_i})
\end{aligned} \tag{8}$$

where  $ds$  is given by Equation (A.3) and  $A_i$  and  $b_i$  are profile specific constants given by Jones<sup>[11]</sup>. The unsteady lift for attached flow is rewritten to include the DTEG deflection given by the unsteady offset of AOA

$$C_L^P = C_{L,\alpha} (\alpha_E - \alpha_{0,E}) + \pi b \frac{\dot{\alpha}}{U}, \tag{9}$$

where higher order terms of heave motion and flow rate given by the unsteady version of Theodorsen<sup>[12]</sup> theory have been neglected.

### C. Lift in stalled flow with trailing edge separation

This work is based on the B-L model which originally deals with both LE vortex shedding and TE separation; however, LE eddy separation is not included in this paper. The static flat plate lift in a Kirchoff flow<sup>[10]</sup> with the DTEG ( $\beta$ ) deflection angle is written as

$$C_L^{st}(\alpha) + \Delta C_{L,DTEG}^{st}(\alpha, \beta) = C_{L,\alpha} \left( \frac{1 + \sqrt{f^{st}(\alpha, \beta)}}{2} \right)^2 [\alpha - \alpha_0(\beta)] \tag{10}$$

The  $\alpha_0$  contains the static AOA offset for a cambered profile plus the DTEG deflection contribution to the AOA offset. The term  $\Delta C_{L,DTEG}^{st}$  marks the stationary DTEG contribution to the lift given by CFD or measurements in a wind tunnel shown in Figure B.1.  $C_{L,\alpha}$  is the slope of the linear region of attached flow at zero  $\beta$ . The  $f^{st}$  determines the steady separation point for the TE separation as defined in Figure 2.

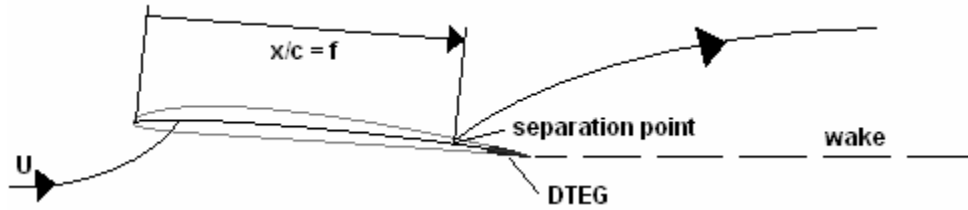


**Figure 2;** trailing edge separation point  $f$  defined in the Kirchoff flow past a flat plate.  
The separation point will also depend on the DTEG.

The flow is fully attached for  $f=1$  and fully separated for  $f=0$ . Assuming that the static lift curve is given, the separation point can be determined as a function of AOA ( $\alpha$ ) and DTEG deflection angle ( $\beta$ ) by inversion of Equation (10).

$$f^{st} = \left( 2 \sqrt{\frac{C_L^{st}(\alpha) + \Delta C_{L,DTEG}^{st}(\alpha, \beta)}{C_{L,\alpha}(\alpha - \alpha_0(\beta))} - 1} \right)^2 \tag{11}$$

There are two issues of the inversion and the representation of the lift. The separation point can firstly not exceed the LE of the airfoil the linear lift slope

$$C_{L,\alpha} = \max \left\{ \frac{C_L^{st}(\alpha)}{\alpha - \alpha_0(\beta = 0)} \right\} \quad (12)$$

It is assumed that the flow in the attached region follows the  $C_{L,\alpha}$  slope. To handle variations in  $(\alpha, \beta)$  exceeding the limits of Equation (11), the separation point is defined as zero for  $(\alpha, \beta)$  values exceeding Equation (13).

$$|C_L^{st}(\alpha, \beta)| = \left| \frac{C_{L,\alpha}(\alpha - \alpha_0(\beta_{\max}))}{4} \right| \quad (13)$$

The lift coefficient for fully separated flow ( $C_L^{fs}$ ) is given by Equation (15)

$$C_L^{st} = C_{L,\alpha}(\alpha - \alpha_0)f^{st} + C_L^{fs}(1 - f^{st}) \quad (14)$$

$$C_L^{fs} = \frac{C_L^{st}(\alpha) + \Delta C_{L,DTEG}^{st}(\alpha, \beta) - C_{L,\alpha}(\alpha - \alpha_0)f^{st}}{1 - f^{st}}, \quad \text{for } f^{st} \neq 1 \quad (15)$$

where  $C_L^{st}$  marks the static lift curve,  $\Delta C_{L,DTEG}^{st}$  the static lift from DTEG and  $f^{st}$  the static separation point given by Equation (11). Equation (15) becomes equal to the static lift for AOA and DTEG deflections beyond Equation (13). For fully attached flow Hansen<sup>[7]</sup> states that Equation (14) must be inserted into (15) to avoid dividing by zero. Consequently the fully separated lift in the attached region yields Equation (16).

$$C_L^{fs}(\alpha, \beta) \rightarrow \frac{C_L^{st}(\alpha, \beta)}{2}, \quad \text{for } f^{st} = 1 \quad (16)$$

Hence, the lift for fully separated flow at low angles of attack is half the lift for fully attached flow.

The suggested step-by-step procedure for finding  $C_{L,fs}$  and  $f^{st}$  is as follows: Find the AOA for zero lift for DTEG deflection at zero degree. Find the maximum linear lift slope for zero DTEG deflection ( $C_{L,\alpha}$ ). Find the min/max limits for use of Kirchoff's static lift for flat plate flow by calculating the maximum AOA offset when using the DTEG, e.g. positive five degree DTEG deflection for maximum  $C_L$  and negative five degree DTEG deflection for minimum  $C_L$ . This is done to avoid dividing with zero in Equation (15). Compute the separation point function  $f^{st}$  from (11) using the original lift curve for profile and DTEG contribution. Finally compute the lift coefficient for fully separated flow (15) but using (16) for the attached flow region.

#### D. Dynamics of the TE separation

Two state variables in the B-L model are used to describe the dynamic behavior of the TE separation. The separation is related to the pressure distribution over the airfoil, and the pressure is related to the lift on the airfoil; for a given lift there is a certain pressure distribution with a certain separation point. It is assumed that there is a time-lag between the pressure and lift modeled as Equation (17) and the dynamics of the boundary layer is modeled as Equation (18).

$$C_L^{p'} = C_L^p \cdot e^{\frac{-ds}{\tau_p}} + C_L^p \left( 1 - e^{\frac{-ds}{\tau_p}} \right), \quad \beta_E' = \beta_E \cdot e^{\frac{-ds}{\tau_p}} + \beta_E \left( 1 - e^{\frac{-ds}{\tau_p}} \right) \quad (17)$$

$$f^{dyn} = f^{dyn} e^{\frac{-ds}{\tau_b}} + f^{st} \left( 1 - e^{\frac{-ds}{\tau_b}} \right) \quad (18)$$

$$f^{st} = f^{st}(\alpha, \beta), \text{ where } \alpha = \frac{C_L^{P'}}{C_{L,\alpha}}, \beta = \beta_E' \quad (19)$$

The time constants  $\tau_p$  and  $\tau_b$  marks the time-lags for the dynamic pressure-lift lag and the dynamics in the buildup/destruction lag of the boundary layer. The  $C_L^{P'}$  is a helping state variable containing the equivalent lift coefficient after the pressure time-lag has been included and  $\beta_E'$  is the effective pressure lagged DTEG deflection angle. Using this semi-dynamic lift coefficient  $C_L^{P'}$  and effective DTEG deflection angle  $\beta_E'$  the pressure lagged separation point  $f^{st}$  is found using Equation (11) and (19). The dynamic separation point is used in the linear interpolation between the full separation lift and the attached flow lift to find the overall dynamic lift with TE separation.

$$C_L^{dyn} = C_{L,\alpha}(\alpha_E - \alpha_{0,E})f^{dyn} + C_L^{fs}(1 - f^{dyn}) + \pi b \frac{\dot{\alpha}}{U} \quad (20)$$

Equation (20) does not include higher order terms given by Equation (A.6), (A.7) or higher order Theodorsen terms for heave motion and flow rate. These terms have been considered and found to be of a magnitude lower than the uncertainty of the wind tunnel measurements performed in the Velux tunnel.

## E. Drag

The unsteady drag is bounded to variations about a static drag curve provided as input to the model. The drag consists of three parts; *Induced drag*, *viscous drag* and *DTEG contribution to drag* modeled as a change in AOA offset similar to the dynamic lift. A description of the *induced drag* is provided by Hansen<sup>[7]</sup>. The *viscous drag* is either calculated using CFD or measured in a wind tunnel. The suggested model assumes that the *DTEG drag contribution* scales with the dynamic separation point function ( $f^{dyn}$ ). This assumption is not validated, but considered valid for the two extreme cases (fully attached flow and fully separated flow). The DTEG contribution to the geometric and effective AOA is included using the DTEG specific helping variables  $\alpha_{3/4,DTEG}$  and  $\alpha_{E,DTEG}$  given in Equation (21).

$$\begin{aligned} \alpha_{3/4,DTEG} &= \alpha_{3/4} - (\alpha_{0,st}^\beta + \alpha_{0,dyn}^\beta) f^{dyn} \\ \alpha_{E,DTEG} &= \alpha_E - (\alpha_{0,E} - \alpha_0^c) f^{dyn} \end{aligned} \quad (21)$$

The original dynamic drag  $C_D^{dyn}$  equation by Hansen<sup>[7]</sup> is otherwise reused. Please refer to the paper by Hansen for details.

$$\begin{aligned} C_D^{dyn} &= C_D^{st}(\alpha_{E,DTEG}) + \Delta C_D^{ind} + \Delta C_D^{f^{dyn}} \\ \Delta C_D^{ind} &= (\alpha_{3/4,DTEG} - \alpha_{E,DTEG}) C_L^{dyn} \\ \Delta C_D^{f^{dyn}} &= (C_D^{st}(\alpha_{E,DTEG}) - C_{D,0}) \left( \left( \frac{1 - \sqrt{f^{dyn}}}{2} \right)^2 - \left( \frac{1 - \sqrt{f^{st}}}{2} \right)^2 \right) \end{aligned} \quad (22)$$

It is assumed that the drag coefficient at zero lift ( $C_{D,0}$ ) is unaffected by the DTEG.

## F. Moment

The unsteady TE separation affects the moment through the traveling of the pressure center due to separation. However as for the drag, the present model binds the unsteady moment, to variations about the static moment curve provided as input. The DTEG contribution to the dynamic moment ( $C_{M,DTEG}$ ), see Equation (A.1-A.7) is added to Equation (23) and scaled by the dynamic separation point  $f^{dyn}$ . As for the drag, the fact of using the separation point to scale the effect of the DTEG contribution to the moment is assumed valid for the two extreme cases (fully attached flow = higher order terms of the Gaunaa DTEG model is included<sup>[4]</sup> and for fully separated flow the suggested model becomes the B-L model<sup>[13]</sup>).

$$C_M^{dyn} = C_M^{st}(\alpha_{E,DTEG}) + \Delta C_M^{f,dyn} + C_{M,DTEG} \cdot f^{dyn} - \pi b \frac{\dot{\omega}}{2U} \quad (23)$$

Please refer to the paper by Hansen<sup>[7]</sup> for details on the term  $\Delta C_M^{f,dyn}$ . A smaller term from the original B-L model has been excluded which was of no importance to the overall results.

## III. Results

**Figure 3** illustrates a comparison between the original B-L and the newly suggested dynamic stall model for both attached flow and stalled flow regimes without DTEG deflection. The purpose for showing this figure is to illustrate the agreement between the original implementation of the B-L model suggested by Hansen<sup>[7]</sup> and the model presented in this paper. In **Figure 4** the Velux measurements of the static lift described by Bak<sup>[8]</sup> is shown and used as input for the results in Figure 5. **Figure 5** illustrates that the lift for the suggested dynamic stall model operates in agreement with the measurements performed in the Velux wind tunnel. For AOA at 4.6 degrees there is a good agreement between measurements, this model, and the original Gaunaa model<sup>[4]</sup> with the exception that for the highest reduced frequency the measurements suggest using a slightly more open loop which may be due to viscous effects not part of the model. For AOA at 18.5 degree in deep stall the DTEG flapping motion creates loops which are well captured by the model, notice how the loop slope is becoming steeper for increased reduced frequency this is also seen in the measurements. The suggested model should be extended to include measurements or CFD calculations of drag and moment coefficients in a similar manner to the way the lift coefficient is adjusted according to static measurements. **Figure 6** shows the static lift, drag and moment coefficients for a 3D corrected Naca63418 profile which is used as input for the results shown in Figure 7 and 8. **Figure 7** combine the pitching and flapping motion in phase, which means the DTEG aides the pitching motion of the profile enlarging the pitching effect. **Figure 8** combines the pitching and DTEG motion in counter phase, which means the DTEG, compensates the pitching motion of the profile. The results shown are given by the suggested model using the DTEG measurements of static lift, drag and moment coefficients on a B1-18 profile as input. This figure clearly illustrates the aerodynamic complexity of combining not only the pitching motion of a profile but also adding a dynamic DTEG deflection motion. Figure 8 suggest that with the chosen pitching and DTEG deflection amplitudes in counter phase the  $C_M$  loop slope at  $AOA=4^\circ$  can be removed and the  $C_L$  slope from pure pitching loop can be halved. It should be noted that the dynamic contribution to drag and moment from actuation the DTEG scales with the dynamic separation coefficient. This scaling causes the effect of using a DTEG to be zero in deep stall with regard to drag and moment; a better approach would be to extend the model to include the DTEG measurements for deep stall scaling of drag and moment as done for the lift.

## IV. Conclusion

A dynamic stall model has been developed which predicts the unsteady aerodynamic forces and moments on an airfoil section undergoing arbitrary motion in heave, lead-lag, pitch, trailing edge flapping. The DTEG deflection angles are limited to plus and minus 5 degrees. For zero DTEG deflections the model becomes equivalent to the original implementation of the B-L model by Hansen<sup>[7]</sup>. When actuating the DTEG the model becomes equal to the Gaunaa model<sup>[4]</sup> in the attached flow region excluding some higher order terms which is part of the original Gaunaa model. For the separated flow region the model becomes a crossover between the two models when using the DTEG. The dynamic lift in stalled and attached region show good agreement with the measurements performed in the Velux tunnel. The model should be extended to scale the DTEG contribution to drag and moment in deep stall in a similar fashion to how the lift is scaled instead of using the simple dynamic separation point scaling.

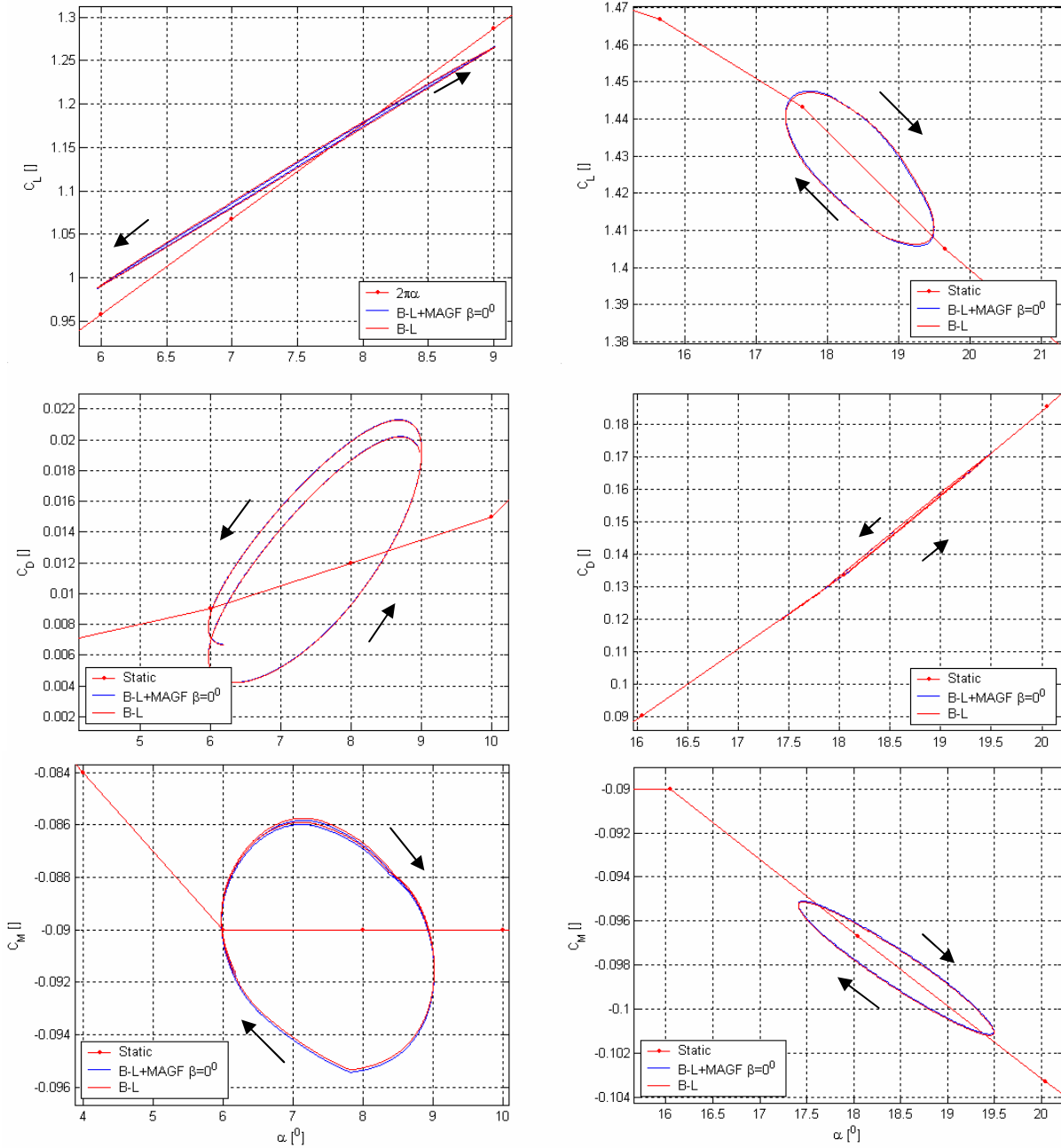


**Figure 3;** comparison between the suggested model of this paper and the original B-L model. The attached flow region comparison is made for  $C_L$  loops at  $\Delta\alpha=6^\circ$  to  $9^\circ$  (top left),  $C_D$  loops at  $\Delta\alpha=6^\circ$  to  $9^\circ$  (middle left) and  $C_M$  loops for  $\Delta\alpha=6^\circ$  to  $9^\circ$  (lower left). The separated flow region comparison is made for  $C_L$  loops at  $\Delta\alpha=17.4^\circ$  to  $19.5^\circ$  (top right),  $C_D$  loops at  $\Delta\alpha=17.4^\circ$  to  $19.5^\circ$  (middle right) and  $C_M$  loops for  $\Delta\alpha=17.4^\circ$  to  $19.5^\circ$  (lower right). For all calculations the DTEG deflection  $\beta=0^\circ$ . The AOA is changed cyclic at a reduced frequency of  $k=\omega c/(2U_0)=0.15$ . Arrows indicate the orientation of the loops in time.

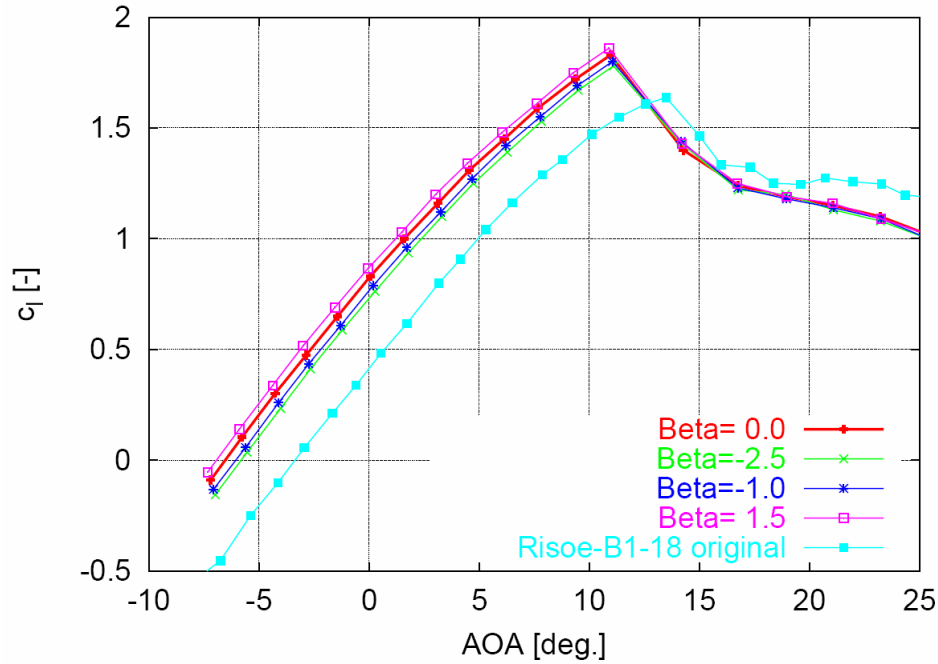


**Figure 4;** measured  $C_L$  (top) values for various AOA and DTEG deflections from Velux described by Bak<sup>[8]</sup>. Static  $C_L$  (bottom) values provided by the model suggested in this paper using the static DTEG  $C_L$  curve from the Velux experiment described by Bak<sup>[8]</sup> see Figure B.1

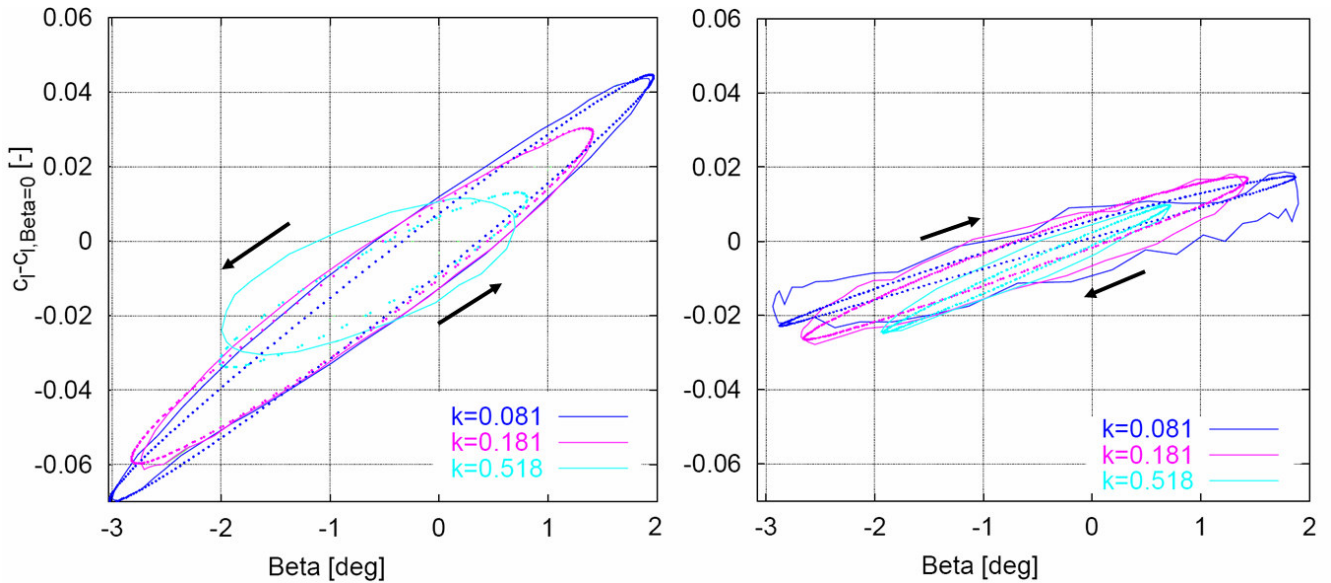


**Figure 5;**  $\Delta C_L$  loops as function of harmonic DTEG deflections at constant AOA  $4.6^\circ$  (left) and  $18.5^\circ$  (right). Lift values are shifted so  $\Delta C_L = 0$  for  $\beta = 0^\circ$ . Full lines shows the measured  $\Delta C_L$  loops from Velux described by Bak<sup>[8]</sup>. Dotted lines represent the presented model. The DTEG deflection  $\beta$  ranges from  $-3^\circ$  to  $1.97^\circ$  for reduced frequency  $k = \omega c / (2U_0) = 0.081$ , for  $\beta = -2.8^\circ$  to  $1.3^\circ$  the  $k = \omega c / (2U_0) = 0.181$  and finally for  $\beta = -2^\circ$  to  $0.76^\circ$  the  $k = \omega c / (2U_0) = 0.518$ . Arrows indicate the orientation of the loops in time.

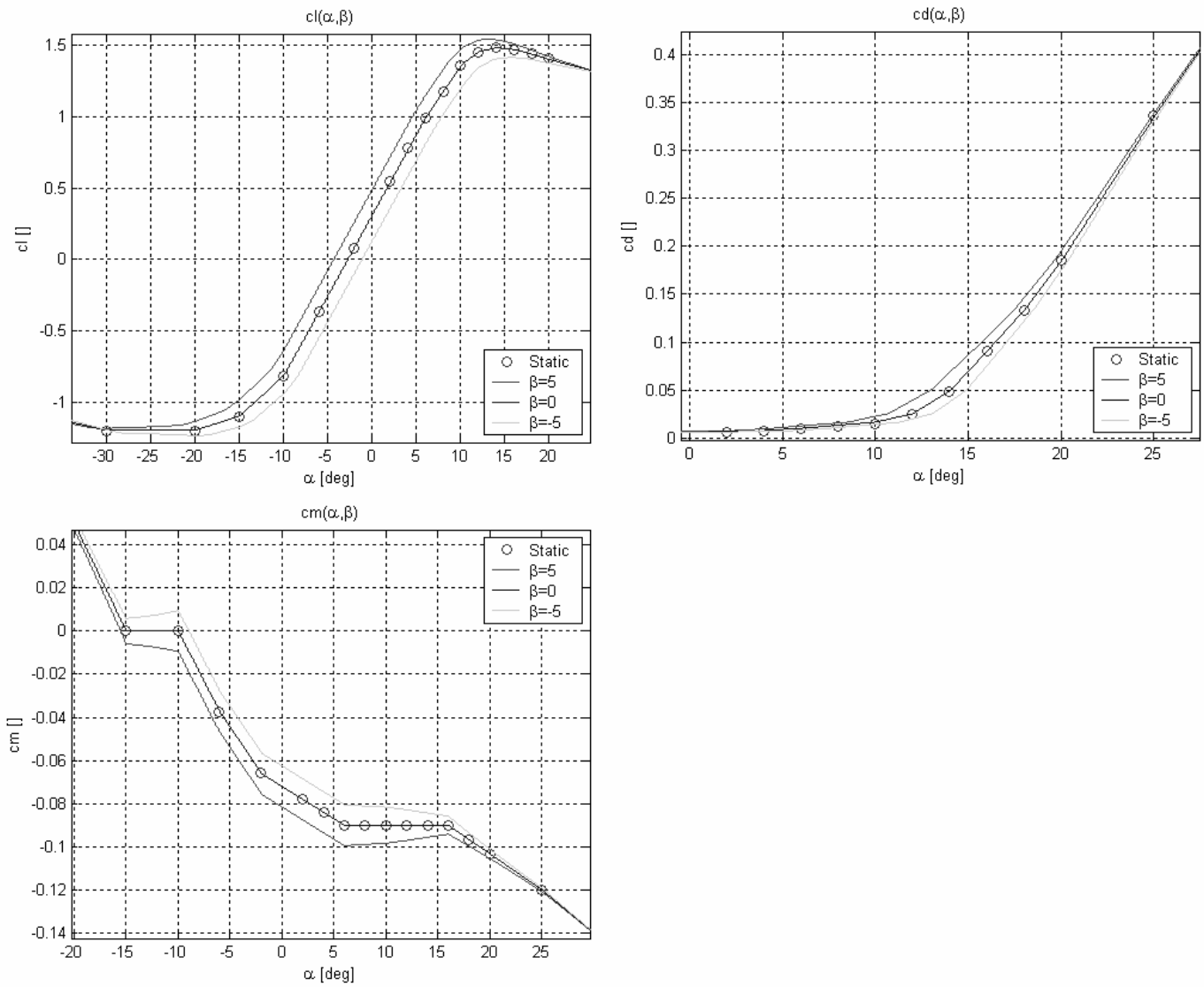


**Figure 6:** static  $C_L$  (top left)  $C_D$  (top right) and  $C_M$  (bottom) for 3D corrected Naca63418 profile with  $\beta = -5^\circ, 0^\circ$  and  $5^\circ$ . Static  $C_L$  (top left) is based on extrapolated static DTEG  $C_L$  curve from the Velux experiment described by Bak<sup>[8]</sup> see Figure B.1.

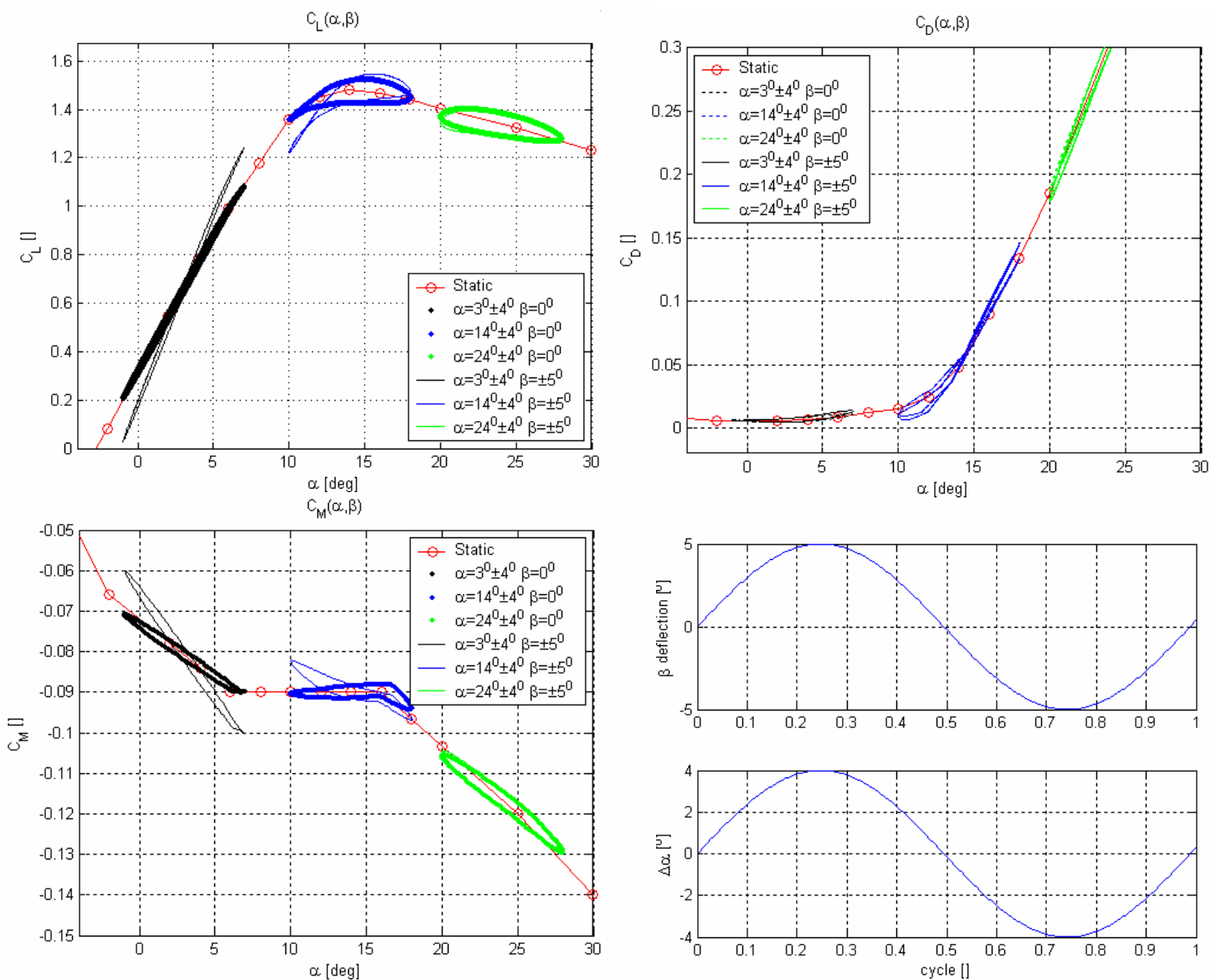


**Figure 7;** Response of  $C_L$ (upper left),  $C_D$ (upper right) and  $C_M$ (lower left) to oscillatory pitching motion without the use of DTEG deflection and with use of DTEG deflection in phase with pitching motion. The results are given by the suggested model using the DTEG measurements of static lift, drag and moment coefficients on a B1-18 profile as input. Reduced frequency is  $k=\omega c/(2U_0)=0.1$ .  $\Delta\alpha=4^\circ$   $\Delta\beta=5^\circ$

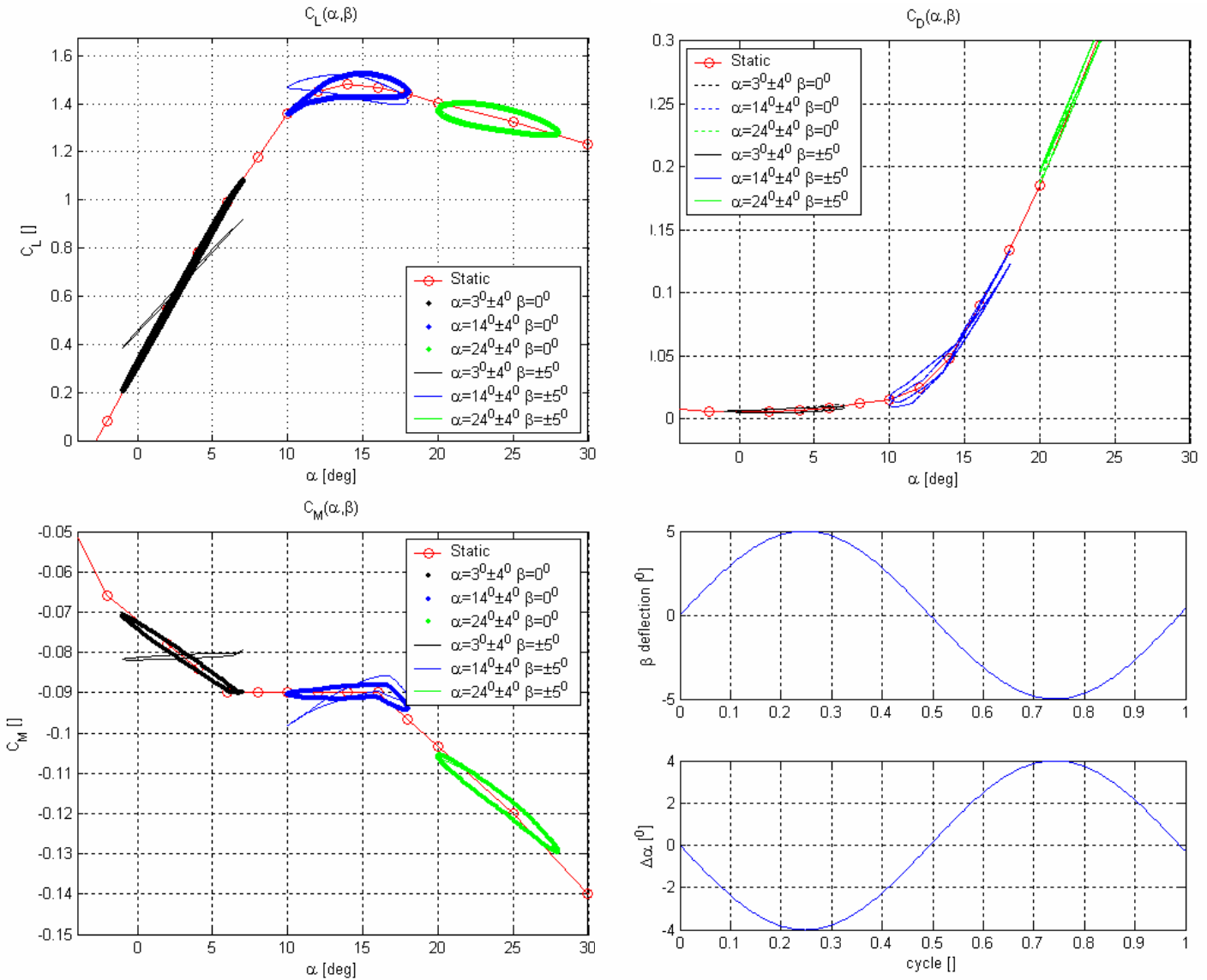


**Figure 8;** Response of  $C_L$ (upper left),  $C_D$ (upper right) and  $C_M$ (lower left) to oscillatory pitching motion without the use of DTEG deflection and with use of DTEG deflection in counter phase with pitching motion. The results are given by the suggested model using the DTEG measurements of static lift, drag and moment coefficients on a B1-18 profile as input. Reduced frequency is  $k=\omega c/(2U_0)=0.1$ .  $\Delta\alpha=4^\circ$   $\Delta\beta=5^\circ$

## References

- <sup>1</sup>Friedmann, P.P., "Rotor-Wing Aeroelasticity: Current Status and Future Trends", AIAA Journal Vol. 42, No. 10, October 2004.
- <sup>2</sup>Troldborg, N., "Computational study of the Risø-B1-18 airfoil with a hinged flap providing variable trailing edge geometry", Wind Engineering, vol. 29, no. 2, 2005
- <sup>3</sup>Buhl, T.; Gaunaa, M.; Bak, C.; "Potential Load Reduction Using Airfoils with Variable Trailing Edge Geometry"; Journal of Solar Energy Engineering; November 2005, Vol. 127, p. 503-516
- <sup>4</sup>Gaunaa, M., "Unsteady 2D Potential-flow Forces on a Thin Variable Geometry Airfoil Undergoing Arbitrary Motion", Risø-R-1478, Risø-DTU, Denmark, June 2004.

<sup>5</sup>Andersen, P.B.; Gaunaa, M.; Bak, C.; Buhl, T., “Load alleviation on wind turbine blades using variable airfoil geometry”. In: Proceedings (online). 2006 European Wind Energy Conference and Exhibition, Athens (GR), 27 Feb -2 Mar 2006. (European Wind Energy Association, Brussels, 2006) 8 p

<sup>6</sup>Abdallah, I.; “Advanced Load Alleviation for Wind Turbines using Adaptive Trailing Edge Geometry: Sensing Techniques”. M.Sc Thesis Project; July 13, 2006, Technical University of Denmark, Department of Mechanical Engineering, Section of Fluid Mechanics

<sup>7</sup>Hansen, M.H.; Gaunaa, M.; Madsen, H.Aa.; “A Beddoes-Leishman type dynamic stall model in state-space and indicial formulations”, Risø-R-1354, Risø-DTU, Denmark, June 2004.

<sup>8</sup>Bak, C., Gaunaa, M., Andersen P.B.; Buhl T.; Hansen P.; Clemmensen K.; Moeller R.; “Wind Tunnel Test on Wind Turbine Airfoil with Adaptive Trailing Edge Geometry”, Paper for conference AAIA-2007-1016, Reno, USA, Jan 2007

<sup>9</sup>von Karman, Th. & Sears, W.R.; “Airfoil Theory for Non-Uniform Motion.”, Journal of the Aerodynamical Science. 5(10) 1938. p.379-390

<sup>10</sup>Thwaites, B.E.; “Incompressible Aerodynamics”, Cambridge University Press, 1961.

<sup>11</sup>Jones, R.T.; “The Unsteady Lift of a Wing of Finite Aspect Ratio”, Tech. Rep. 681, NACA Report, 1940.

<sup>12</sup>Theodorsens, T.; “General Theory of Aerodynamic Instability and The Mechanism of Flutter,” NACA Report 496, 1935, pp. 413-433.

<sup>13</sup>Leishman, J.G.; Beddoes, T.S.; “A Generalized Model for Airfoil Unsteady Aerodynamic Behavior and Dynamic Stall Using Indicial Method,” Proceedings of the 42<sup>nd</sup> Annual Forum of the American Helicopter Society, Washington D.C. June 1986.

## Appendix

### A. DTEG Equations

Kelvin theorem states that the change in global circulation for an unsteady potential-flow solution is zero for a 2D universe. A step change in DTEG will cause a change in the circulation around the profile, in order to keep the global circulation constant an eddy is shed downstream as illustrated in Figure A.1.

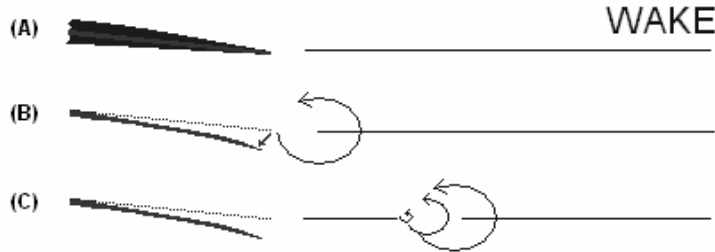


**Figure A.1:** eddies shed and transported downstream (C) in the unsteady wake when the DTEG is activated (B)

The effective three-quarter downwash is termed  $QC$  in the work of Gaunaa it will be termed  $w_\beta^E$  in this paper. Von Karman<sup>[9]</sup> showed how the effect of an unsteady near wake can be added to the three-quarter downwash using the indicial function concept (A.1). The aerodynamic state variable  $y_i$  is given by (A.1).

$$w_\beta^E = w_\beta \left( 1 - \sum_i A_i \right) + \sum_i y_i \quad (\text{A.1})$$

$$y_i = y_i \cdot e^{-ds \cdot b_i} + A_i w_\beta (1 - e^{-ds \cdot b_i}) \quad (\text{A.2})$$

The non-time step  $ds$  is given by (A.3)

$$ds = \frac{1}{b} \int_t^{t+\Delta t} \overline{U}(t') dt' \quad (\text{A.3})$$

$A_i$  and  $b_i$  are profile specific constants provided by Jones<sup>[11]</sup>. Once the effective three-quarter downwash ( $w_\beta^E$ ) is known the DTEG contribution to the normal ( $C_{N,DTEG}$ ) and tangential force ( $C_{T,DTEG}$ ) can be found along with the contribution to the moment ( $C_{M,DTEG}$ ), see the following equations

$$C_{N,DTEG} = \frac{b}{\pi \bar{U}^2} \left( \ddot{\beta} F_{y,2} + \dot{\beta} F_{dyd\epsilon,2} \bar{U} - \beta F_{dyd\epsilon,2} \dot{U}_x \right) + 2\pi \frac{w_\beta^E}{\bar{U}} \quad (\text{A.4})$$

$$C_{T,DTEG} \cdot \bar{U}^2 = \left| \begin{aligned} & \frac{\pi}{2} \left( 2w_{fullflap}^E - \dot{\alpha} b + \frac{\dot{U}_y}{2\pi} (K_{dydx,1} + H_{dydx,1} + \beta K_{dydx,2} + \beta H_{dydx,2}) + \frac{\dot{\beta}}{2\pi} (K_{y,2} + H_{y,2}) \right)^2 \\ & - \frac{\pi}{2} \left( 2w_{noflap}^E - \dot{\alpha} b + \frac{\dot{U}_y}{2\pi} (K_{dydx,1} + H_{dydx,1}) \right)^2 \\ & + 2b\beta \cdot TI1_2 (\dot{U}_y - ab\dot{\alpha}) \\ & + \frac{b}{\pi} \ddot{\beta} (TI2_{2,1} + \beta \cdot TI2_{2,2}) \\ & - \frac{b}{\pi} \dot{U}_y \beta (TI3_{2,1} + TI3_{1,2} + \beta \cdot TI3_{2,2}) \\ & + \frac{b}{\pi} \bar{U} \dot{\beta} \cdot TI3_{2,1} \\ & + b^2 \dot{\alpha} \beta \cdot TI4_2 \\ & - 2\bar{U} [w_{fullflap}^E (TI5_1 + \beta TI5_2) - w_{noflap}^E \cdot TI5_1] \\ & - b\bar{U} \dot{\alpha} \beta \cdot TI6_2 \\ & + \frac{\bar{U}^2}{\pi} \beta (TI8_{2,1} + TI8_{1,2} + \beta \cdot TI8_{2,2} - H_{dydx,1} \cdot TI7_2 - H_{dydx,2} TI7_1 - \beta \cdot H_{dydx,2} TI7_2) \\ & + \frac{\bar{U}}{\pi} \dot{\beta} (TI9_{2,1} + \beta \cdot TI9_{2,2} - H_{y,2} (TI7_1 + \beta \cdot TI7_2)) \end{aligned} \right. \quad (\text{A.5})$$

$$C_{N,DTEG}^{dyn} = \frac{b}{\pi \bar{U}^2} \ddot{\beta} F_{y,2} + \frac{b}{\pi \bar{U}} \dot{\beta} F_{dyd\epsilon,2} \quad (\text{A.6})$$

$$C_{T,DTEG}^{dyn} = \left| \begin{aligned} & \frac{\pi}{2\bar{U}^2} \left( \frac{\dot{\beta}}{2\pi} (K_{y,2} + H_{y,2}) \right)^2 \\ & + \frac{b}{\pi \bar{U}^2} \dot{\beta} \cdot TI2_{2,1} \\ & + \frac{b}{\pi \bar{U}} \dot{\beta} \cdot TI3_{2,1} \\ & + \frac{1}{\pi \bar{U}} \dot{\beta} (TI9_{2,1} - H_{y,2} TI7_1) \end{aligned} \right. \quad (\text{A.7})$$

$$C_{M,DTEG} \bar{U}^2 \pi = \begin{cases} b \dot{U}_x \beta (G_{dydx,2} - a \cdot F_{dydx,2}) \\ + \bar{U}^2 \beta (F_{dydx,2} + H_{dydx,2}) \\ - b \bar{U} \dot{\beta} (G_{dydx,2} - a \cdot F_{dydx,2}) \\ + \bar{U} \dot{\beta} \cdot F_{y,2} \\ 0.5 \pi \dot{\beta} \cdot H_{y,2} \\ - b \ddot{\beta} (G_{y,2} - a \cdot F_{y,2}) \\ + 2 \pi^2 \bar{U} (0.5 + a) (w_\beta^E) \\ - C_{N,DTEG} \cdot \pi \bar{U}^2 \end{cases} \quad (\text{A.8})$$

For the constants  $T11$ ,  $T12$ ,  $T13$ ,  $T14$ ,  $T15$ ,  $T16$ ,  $T17$ ,  $T18$ ,  $T19$ ,  $F$ ,  $G$  and  $K$  please refer to Gaunaa<sup>[4]</sup>. The notation  $(\dot{\quad})$  marks the derivative with respect to time.

### B. Measured DTEG static lift curve

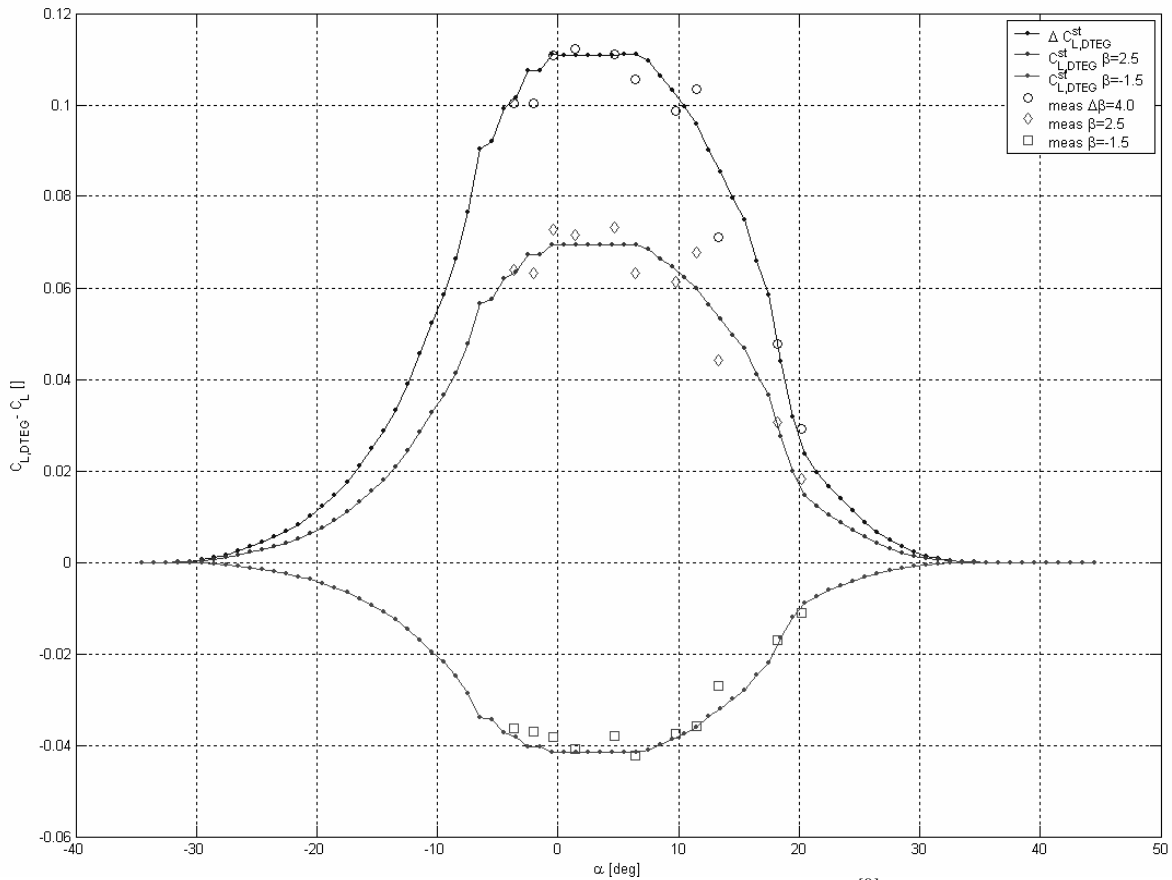


**Figure B.1;** wind tunnel measurements of a DTEG described by Bak<sup>[8]</sup>,  $Re=1.66$ million deflections at  $-1.5$  and  $2.5$  degree at various AOA for a Risø-B1-18 profile. The lines indicate fitted  $\Delta C_{L,DTEG}^{st}$  curves as function of AOA and DTEG deflections.